WILEY | Hindawi

Research Article

Establishment of Dynamic Evolving Neural-Fuzzy Inference System Model for Natural Air Temperature Prediction

Suraj Kumar Bhagat [iD],[1] Tiyasha Tiyasha [iD],[1] Zainab Al-khafaji [iD],[2] Patrick Laux [iD],[3] Ahmed A. Ewees [iD],[4,5] Tarik A. Rashid [iD],[6] Sinan Salih [iD],[7] Roland Yonaba [iD],[8] Ufuk Beyaztas [iD],[9] and Zaher Mundher Yaseen [iD][10]

[1]*Faculty of Civil Engineering, Ton Duc Thang University, Ho Chi Minh, Vietnam*
[2]*Building and Construction Techniques Engineering Department, AL-Mustaqbal University College, Hillah 51001, Iraq*
[3]*Institute of Meteorology and Climate Research (IMK-IFU), Karlsruhe Institute of Technology, Campus Alpin,
Garmisch-Partenkirchen, Germany*
[4]*Department of Information Systems, College of Computing and Information Technology, University of Bisha,
Bisha 61922, Saudi Arabia*
[5]*Department of Computer, Damietta University, Damietta, Egypt*
[6]*Computer Science and Engineering Department, University of Kurdistan Hewler, Erbil, KRI, Iraq*
[7]*Artificial Intelligence Research Unit (AIRU), Dijlah University College, Al-Dora, Baghdad, Iraq*
[8]*Laboratoire Eaux, Hydro-Systèmes et Agriculture (LEHSA),
Institut International D'Ingénierie de L'Eau et de L'Environnement (2iE), 01 P. O. Box 594, Ouagadougou 01, Burkina Faso*
[9]*Department of Statistics, Marmara University, Istanbul, Turkey*
[10]*Civil and Environmental Engineering Department, King Fahd University of Petroleum and Minerals, Dhahran 31261,
Saudi Arabia*

Correspondence should be addressed to Roland Yonaba; roland.yonaba@gmail.com

Air temperature (AT) prediction can play a significant role in studies related to climate change, radiation and heat flux estimation, and weather forecasting. This study applied and compared the outcomes of three advanced fuzzy inference models, i.e., dynamic evolving neural-fuzzy inference system (DENFIS), hybrid neural-fuzzy inference system (HyFIS), and adaptive neurofuzzy inference system (ANFIS) for AT prediction. Modelling was done for three stations in North Dakota (ND), USA, i.e., Robinson, Ada, and Hillsboro. The results reveal that FIS type models are well suited when handling highly variable data, such as AT, which shows a high positive correlation with average daily dew point (DP), total solar radiation (TSR), and negative correlation with average wind speed (WS). At the Robinson station, DENFIS performed the best with a coefficient of determination (R^2) of 0.96 and a modified index of agreement (md) of 0.92, followed by ANFIS with R^2 of 0.94 and md of 0.89, and HyFIS with R^2 of 0.90 and md of 0.84. A similar result was observed for the other two stations, i.e., Ada and Hillsboro stations where DENFIS performed the best with R^2: 0.953/0.960, md: 0.903/0.912, then ANFIS with R^2: 0.943/0.942, md: 0.888/0.890, and HyFIS with R^2: 0.908/0.905, md: 0.845/0.821, respectively. It can be concluded that all three models are capable of predicting AT with high efficiency by only using DP, TSR, and WS as input variables. This makes the application of these models more reliable for a meteorological variable with the need for the least number of input variables. The study can be valuable for the areas where the climatological and seasonal variations are studied and will allow providing excellent prediction results with the least error margin and without a huge expenditure.

1. Introduction

One of the commonly measured weather parameters is the air temperature (A_T), which measures the relative motion/ kinetic energy of the component gases that constitute air. It increases when the molecules of a gas are moving more quickly and vice versa. A_T estimation is an important process for several applications, such as in studying vector-borne diseases [1, 2], weather forecasting, climate change [3–5], epidemic forecasting [6], veterinary uses, radiation [7], and heat flux estimation [8], estimation of water potential and vapour pressure deficit [9, 10], ecology [11–13], wastewater treatment [14–16], hydrology [17], urban land use, and urban heat island [18]. The estimation of A_T is usually conducted by weather metrological stations and is considered an essential weather parameter, which is usually measured with high accuracy [19].

1.1. Application of Classic Machine Learning Models.
Improvement of the accuracies of various high-impact weather prediction models using machine learning (ML) models have been the focus of most research activities recently [20–23]. This is based on the nonreliance of ML models on input variables' multicollinearity; hence, they can process numerous input variables [24]. The development of ML-based models for a multitude of stations is achievable and as such, it is possible to monitor the spatial distribution of the prediction such as A_T, when the ML models are fed with spatially continuous input parameters [25, 26]. The postprocessing of the hourly temperature outputs of the Advanced Regional Prediction System (ARPS) using an artificial neural network (ANN) has been investigated by Marzban [27]. The study achieved an average of 40% decline in the mean squared error (MSE) for the validated weather stations. Various ANN-based models for A_T prediction during winter periods have been developed by Jain et al. [28]. The training of the developed models involved the use of patterns that included 6-hours of previous weather information, such as WS, relative humidity (RH), A_T, time of the day, and TSR. In another study by Jang et al. [29], the authors predicted A_T in Southern Quebec (Canada) based on the use of the ANN model and AVHRR images. The employed ML model was trained using Levenberg–Marquardt backpropagation (LM-BP) while the LM-BP was improved using the early stopping method to ensure the generalization of the learning process of the networks. As per Smith et al. [30], the prediction performance of A_T models during winter periods can be improved by incorporating seasonal information in the input pattern, followed by an extension of the duration of previous data to at least 24 hours. The monthly mean A_T prediction performance of ANN and Support Vector Regression (SVR) have been studied by Salcedo-Sanz et al. [31] based on the previously measured values in New Zealand and Australia. The models were also used to predict the climate indices of importance within the studied region. From the results, the SVR model outperformed the ANN model in terms of prediction performance. However, the authors reported that

last years of the test set do not allow the consistency of the prediction performance of different algorithms due to the high fluctuations. Various models, ranging from simple correction (i.e., mean bias) to ML models (such as ANN and random forest (RF)), have been investigated by Eccel et al. [32] for improving the minimum A_T prediction performance of two numerical models for weather prediction. The outcome of the comparative study showed that the RF model in comparison to the other models achieved the best performance in terms of being easier to automate. An establishment of ANN-based models for A_T prediction has been developed by Smith et al. [33]. The models were developed for A_T prediction throughout the year using the data collected since 2005. The ability of the polynomial neural network to bias-correct the National Oceanic and Atmospheric Administration (NOAA) mesoscale model for hourly A_T prediction has been reported by Vashani et al. [34] while another study by Şahin [35] reported monthly mean A_T prediction using remote sensing dataset and ANN model in 20 Turkish cities. The performance of the developed ANN model in monthly mean A_T modelling using remote sensing data was reported as efficient and accurate. Moreover, deciding those hyperparameters is challenging to the nonstationary data.

1.2. Application of Hybrid Machine Learning Models.
The trend of hybrid model application is growing year by year as per its scientific advantages and higher robustness. The ANFIS and ANN models have been evaluated for effectiveness in long-term monthly AT prediction at 30 Iraqi weather stations Kisi and Shiri [36]. The models were trained using the monthly data of 20 weather stations while the data for the remaining 10 stations were used for model validation. The models were also compared against each other in terms of prediction performance and the outcome showed that the ANN model performed better than the ANFIS model in the test period. Moreover, the authors suggested further investigations with other techniques and data management scenarios for the generalization of the application such as other important climatologic variables. Besides, a couple of studies applied a hybridization of adaptive neurofuzzy inference system with optimization methods using mutation Salp Swarm Algorithm as well as Grasshopper Optimization Algorithm (ANFIS-mSG) and particle swarm optimization (ANFIS-PSO) to simulate the soil temperature using univariate independent variables and the high-strength concrete shear strength using multiple independent variables [37, 38]. Both studies reported marginal performance gains compared to the performance of the ANFIS standalone model. Also, both studies reported the hybrid model is limited to the univariate, i.e., AT scenario, and needs to use more derivative data from the primary character. The study by Yi et al. [39] focused on improving the AT prediction accuracy of the Local Data Assimilation and Prediction System (LDAPS) model used in Seoul, South Korea. The study deployed SVR and linear regression models for this purpose and found that the prediction accuracy of the SVR model was higher

than that of the linear regression model. A hybrid model consisting of a regularized extreme learning machine (RELM) and a global climate model has been presented by Shin et al. [40] for seasonal prediction of field-scale daily mean AT. The hybrid model was found capable of performing accurate long-term field-scale AT prediction. The authors advised examining the appropriateness of other regression models to replace the base model. Besides, this can be applied for long-range prediction of other meteorological variables, such as solar radiation, humidity, and rainfall, which are critical meteorological variables in agricultural management. The use of various models (RF, SVR, ANN, and a multimodel ensemble (MME)) to correct the output of LDAPS models when predicting 2-day maximum and minimum AT in South Korea has been reported by Cho et al. [41]. From the results of the analysis, the MME model achieved the best generalization compared to the other three single ML models. Also, the authors suggested applying a more refined ensemble technique (i.e., weighted) for operational purposes. Moreover, [42] applied DENIFS for modelling coagulant dosage rates using an online and offline approach. The authors selected 6 features to perform that and found online approach stands alone as per R (0.80).

1.3. Research Motivation. Following the reported literature on the AT simulation, the implementation of ML models has progressed remarkably over the past decade. Yet, there is no single generalized ML that can be applied for diverse regional characteristics. Conceptually, AT phenomena highlight stochastic and nonstationary process as it is highly correlated with several synoptic climate features and hydrometeorological parameters. The introduction of a new ML model for AT is still an interesting topic for hydrology and climate scientists. Investigation of new paradigms that are reliable and robust in mimicking the AT trends is an open research domain. Thus, the current research has selected three stations, i.e., Robinson, Ada, and Hillsboro located in the USA where AT was predicted by implementing three advanced fuzzy inference system models which are ANFIS, DENFIS, and HyFIS. The selection of those three different meteorological stations is to test the feasibility of the proposed more with the variant trend of AT as those stations are located in different coordinates. Also applying the long-range prediction of other meteorological variables, such as solar radiation and others as a feature to predict AT, is the necessity of the research. Worth to mention, DENFIS and HyFIS models were modelled over the literature for different hydrometrological parameters and confirmed their feasibility such as pan evaporation [43], rainfall [44, 45], evapotranspiration [46], land surface temperature [47], crops suitability [48], and energy consumption [49].

1.4. Research Objectives. The main motivation of the current research is to investigate advanced inference system models for AT prediction. To the best of our knowledge, application of that neurofuzzy algorithm especially DENFIS in the field of AT of the specific location has never been used. The modelling procedure was adopted based on the construction of different input combinations to predict AT. The paper has been divided into four sections: The first section covers the introduction which is followed by the methodology section comprising data description, model concept, and statistical analysis. The third section covers the results and discussions based on statistical analysis done among the models and for three station datasets. Section four presents the conclusion along with recommendations for future studies.

2. Materials and Methods

This section has displayed the explanation of the simulated dataset and the applied predictive models for the A_T prediction.

2.1. Dataset Overview. In the current research, North Dakota (ND) is selected as the case study site for the A_T prediction. The climate of this region is featured by climatic variation and land use-land cover changes due to biofuel production. It is situated in the central northern great plain of North America and can be distributed into our ecoregions, i.e., the lake of Agassiz plain, the northern glaciated plains, the north-western glaciated plain, and the north-western great plains [50]. As per the fourth national assessment report published in 2018, the northern great plains present a challenge for researchers because of their intense changes in elevation throughout the area leading to geological, ecological, and climatological fluctuations. Besides, due to the substantial increment in the temperature and change in precipitation pattern over the last decades. These climate changes may lead to an increase in temperature up to 2°F–4°F by 2050 [51]. The study has selected daily data for three stations at ND from 2015 to 2019. The selected station includes Robinson situated in the southern part of ND at latitude 47° 8′ 35.1384″, longitude −99° 46′ 44.8644″, and an elevation of 1829 m a.s.l., the second is Ada located at latitude 47° 19′ 15.96″, longitude −96° 30′ 50.04″, and an elevation of 910 m a.s.l., and Hillsboro is at latitude 47° 21′ 10.8″, longitude −96° 55′ 19.2″, and an elevation of 886 m a.s.l., as shown in Figure 1.

The study has selected four metrological characteristics of the selected areas for modelling which are average A_T expressed in degree Fahrenheit (°F), average dew point (DP) expressed in °F, total solar radiation (TSR) expressed in Langley (Ly), and average wind speed (WS) expressed in meters per hour (mph). The dataset used for stations has a sample of size $n = 1827$ and the descriptive statistics are presented in Table 1. Furthermore, Figure 2 presents the correlation analysis between the variables for three stations. As per Figure 2, A_T shows a high positive correlation with DP which is 0.98, 0.97, and 0.97 for Robinson (see Figure 2(a)), Ada (see Figure 2(b)), and Hillsboro (see Figure 2(c)) station, respectively. Similarly, the results show that WS is negatively correlated, such as −0.13, −0.18, and −0.27 for Robinson, Ada, and Hillsboro station, respectively.
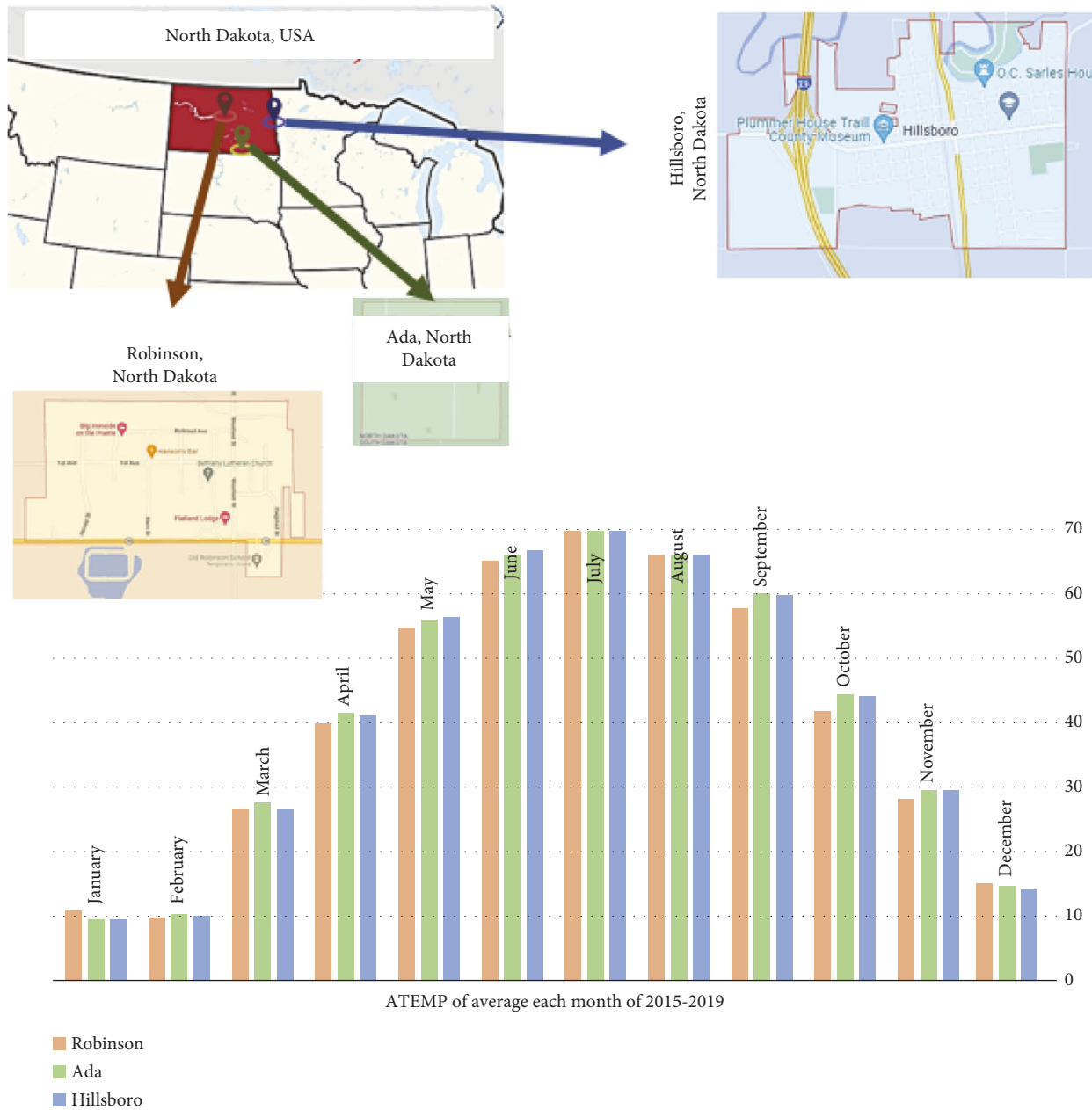
Figure 1: Study area: Ada, Hillsboro, and Robinson stations, North Dakota, North America.

2.2. Applied Predictive Models. The proposed methodology is displayed in the form of a flowchart and presented in Figure 3. Figure 3 shows three interferences in fuzzy AI predictive models. While several attempts attain to score, the best hyperparameters for the rule-based nodes of the fuzzy AI algorithms established the best target values. A detailed explanation of each method is given in the following subsections.

The individual result analysis shows that DENFIS has the highest R^2 (0.968) values when plotted in the scattered diagram (see Figure 8(a)) in comparison to ANFIS (R^2 0.949) and HyFIS (R^2 0.903) performance shown in Figures 8(b) and 7 at Robinson station. In addition to that, it is worth mentioning that Figure 8(c) shows scattered results and in

some cases far from the trend line. The accuracy of the models was also evaluated in terms of Nash and MD and DENFIS performance was excellent during both the training and validation phase (Nash: 0.968 and MD: 0.919). This study has used a modified version of the Willmott formula to overcome the issues created by the presence of the outliers in the dataset which helped the study to better evaluate the model performance.

Thus, DENFIS showed the highest fitness for the Robinson station with the least prediction error (i.e., MAE) for all the considered models. The model error rates were near zero with the least outliers which shows it can handle such data with more ease than others. The scatter plot also supports the conclusion which shows the least variation

TABLE 1: Descriptive statistical parameters for the selected variables in the applied dataset for the analytical approach for the applied models fit.

| Parameters	AT	DP	TSR	WS
Mean	40.65	32.32	13.77	9.42
Standard error	0.55	0.50	0.19	0.10
Median	43.23	32.80	12.62	8.61
Mode	60.99	58.88	6.57	5.86
Standard deviation	23.56	21.43	8.07	4.47
Sample variance	555.51	459.50	65.26	20.06
Kurtosis	−0.76	−0.46	−1.17	2.31
Skewness	−0.41	−0.45	0.33	1.19
Range	110.65	106.52	30.15	34.99
Minimum	−27.22	−33.26	0.98	0.95
Maximum	83.43	73.26	31.12	35.94
Sum	74241.17	59017.50	25159.40	17202.90
Count	1826.00	1826.00	1826.00	1826.00
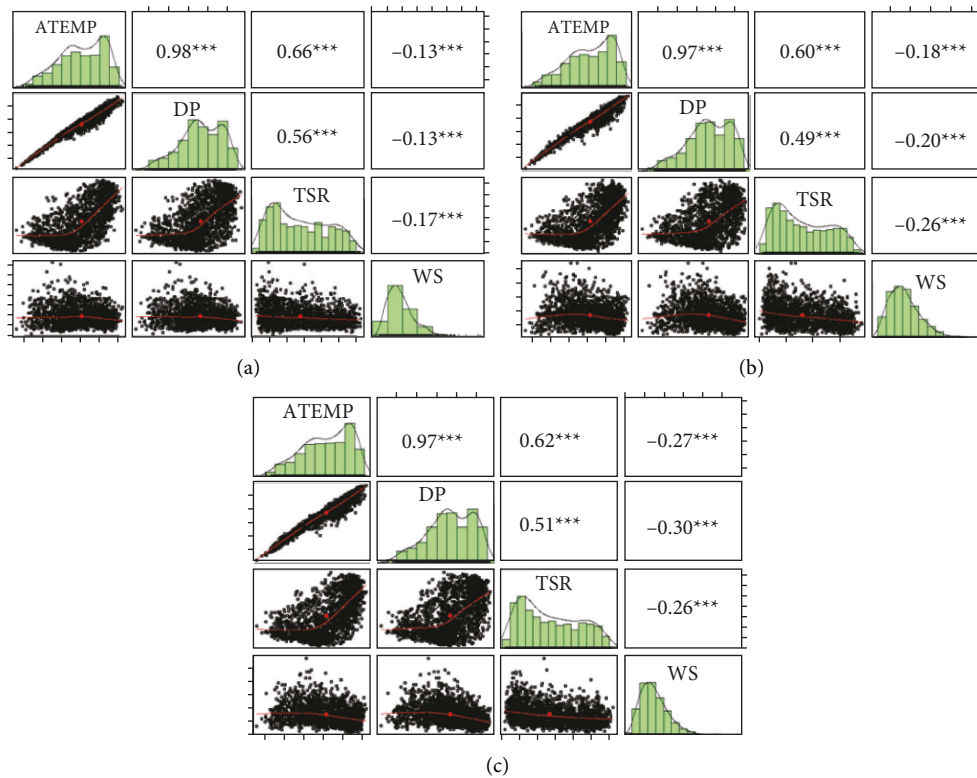
FIGURE 2: Statistical analysis of the applied dataset in terms of pairs plot for (a) Robinson station; (b) Ada station; (c) Hillsboro station.

from the trend line whereas the ANFIS plot is broader and HyFIS predicted values for A_T were scattered and disordered. Even though all the three models' training and validation result variation is about 10%, DENFIS was able to produce a consistent result compared to ANFIS and HyFIS.

2.2.1. Dynamic Evolving Neural-Fuzzy Inference System (DENFIS).

One of the recently developed versions of neurofuzzy models is the dynamic evolving neural-fuzzy inference system (DENFIS) which, according to [52], is an extended version of the original evolving fuzzy neural networks (EFuNN). DENFIS is one of the emerging connectionist systems and its structural arrangement stemmed from the original NF models in terms of the arrangement in various layers while a block of rules made up the main core [53]. A major attribute of DENFIS is the use of a clustering procedure for input space partitioning, which is done in the original NF model using various clustering techniques, such as fuzzy c-mean clustering and grid partition (GP), subtractive clustering, etc. DENFIS relies on the so-called evolving clustering method (ECM) for input space partitioning into various regions [54, 55]. Furthermore, DENFIS uses only Takagi-Sugeno-Kang for fuzzy rule base system and triangular fuzzy membership functions (MFs) generation [56]. A recursive clustering
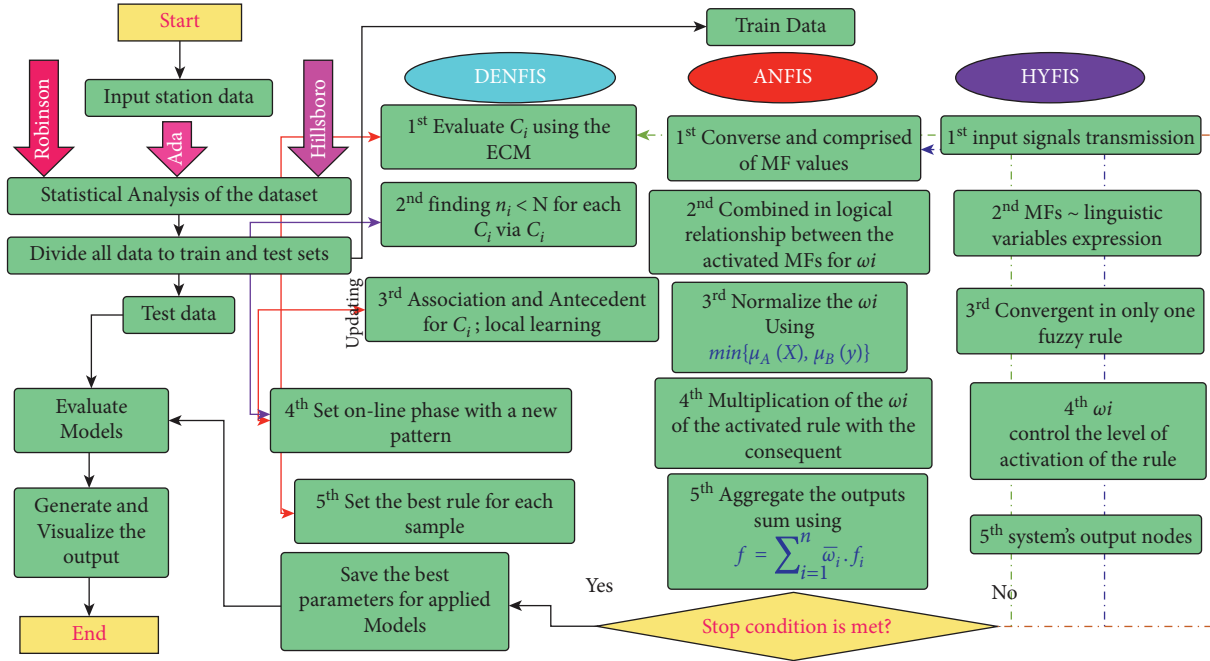
FIGURE 3: The proposed methods for the interferences fuzzy predictive models, statistical evaluators for three-station data, i.e., Robinson, Ada, and Hillsboro stations.

algorithm is used to create the rule bases. The DENFIS model can be mathematically expressed as in (1) and (2) [57]; thus:

$$\text{Rule1: if } X_1 \text{ is } R_{11} \text{ and } X_2 \text{ is } R_{12}, \dots, X_q \text{ is } R_{1q} \text{ then y is } f_1\left(X_1, X_2, X_2, \dots, X_q\right), \tag{1}$$

$$\text{Rule2: if } X_1 \text{ is } R_{21} \text{ and } X_2 \text{ is } R_{22}, \dots, X_q \text{ is } R_{2q} \text{ then y is } f_2\left(X_1, X_2, X_2, \dots, X_q\right), \tag{2}$$

where the predictor or input variable is represented by X_i while y represents the model output or dependent variable; R_{ij} represents the fuzzy sets while the consequent aspect of the fuzzy rules is represented [52, 54]. In the standard NF models, there is a fixed number of fuzzy rules which does not change during the training process, but in the DENFIS model, the fuzzy rules are generated, meaning that only the MFs parameters can change [52, 54]. As such, the calculation of the output of the DENFIS model only considers an aspect of the fuzzy rule base called activated rules [52, 54]. The first phase of the training process of DENFIS is the use of the ECM to cluster the input space and build the fuzzy rules. This involves two major steps which are (i) the first is formation of the antecedent part of the rules via finding the best MFs combination that will activate the cluster centre and improve the MFS efficiency; hence, the selection and formation of the antecedent part are achieved; (ii) the second part is to use the least mean estimation method to fix the consequent part of the fuzzy rules in consideration of the existing pattern within the cluster; hence, one cluster is used for each rule [52, 54, 58]. The DENFIS model involves the following steps [59]: (i) presentation of the first N samples

and establishment of the cluster centre using the ECM, (ii) searching and finding $n_i < N$ example for each cluster centre C_i via closely linking to one of the cluster centers C_i, (iii) association of the fuzzy rules to the C_i with equality (rules = cluster), followed by creation of the antecedent aspects of the rules, (iv) local learning approach-based calculation of the antecedent linear parameters, (v) initiation of the first online phase with a new pattern presentation, (vi) updating the cluster partition using step (iii), (vii) creation of a new rule upon the establishment of a new cluster, followed by creation of the new consequent part, (viii) updating the linear parameters upon creation of a new cluster, (ix) carrying out the required adaptation of the related parameters, and (x) finally, reverting to step (v) for each new sample. The architecture of DENFIS is shown in Figure 4.

2.2.2. Adaptive Neurofuzzy Inference System (ANFIS).
Numerous computational techniques exist which combine artificial neural networks with fuzzy systems to form new systems that are generically referred to as neurofuzzy systems [60]. The study by Jang [61] developed the ANFIS
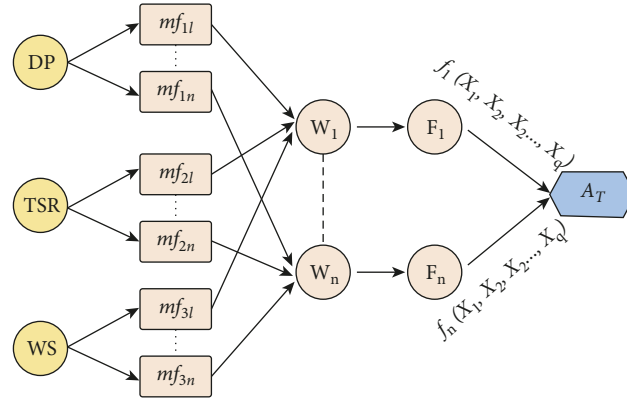
FIGURE 4: A schematic diagram for working flow of the DENFIS algorithm for the specific dataset.

model as a popular variant of the neurofuzzy system which mimics the human way of reasoning by combining the Takagi-Sugeno fuzzy inference systems with the RBF neural network [62]. Neurofuzzy systems rely on decision rules and fuzzy sets to deal with the impreciseness of input data and domain knowledge; it also allows quick approximation of the expected solutions [63]. Hence, these intelligent systems perform well in function approximation, real-time applications, pattern classification, etc. [60, 64]. The architecture of ANFIS is shown in Figure 5.

The fuzzification of the mode input values (x and y) is the objective in Layer 1; this implies the conversion of a set of numerical values into the equivalent fuzzy sets [65]. In this layer, the output is comprised of a set of membership values that correspond to the activation level of each MFs of the input variables: $\{\mu_{A1}(X), \ldots, \mu_{Am}(X)\}$ and $\{\mu_{B1}(y), \ldots, \mu_{B2}(y)\}$. Each node in Layer 2 corresponds to the previous part of the inference rule and depicts the likely combinations between the MFs of the first layer. In this layer, the objective is to establish the logical relationships between the activated MFs for the weight (ω_i) of each rule to be determined. The activation degree of each inference rule is calculated by applying a t-norm operator, such as minimum or algebraic product, as captured, respectively, in equations (1) and (2) discussed earlier. The objective in Layer 3 is to normalize the weights of the activated rules using equation (3) [61, 66].

$$\min\{\mu_A(X), \mu_B(y)\}, \tag{3}$$

$$\mu_A(X) \cdot \mu_B(y), \tag{4}$$

$$\overline{\omega}_i = \frac{\omega_i}{\omega_1 + \cdots + \omega_i + \cdots \omega_n}. \tag{5}$$

A set of adaptive nodes is made up of Layer 4; these nodes represent the inference rule's consequents and provide each rule's outputs. A linear function or a constant value is used to represent each consequent. In the first case, the parameters of the function are the crisp values of the input variables (x and y); the computation of the output of each Layer 4 node 4 is achieved via multiplication of the weight of the activated rule with the consequent. Lastly, Layer 5 aggregates the outputs of each node of Layer 4 nodes

(using equations (4) and (5)) by computing the weighted sum; this provides the final system output as in equation (6) [61, 67].

$$f = \sum_{i=1}^{n} \overline{\omega}_i \cdot f_i. \tag{6}$$

2.2.3. Hybrid Neural-Fuzzy Inference System (HyFIS). There are two learning phases in the HyFIS [68]. Phase one is structure learning which involves the use of the knowledge acquisition module to establish the rules. Phase two is the learning of the parameters for tuning the fuzzy MFs [69] to ensure the expected level of performance will be achieved. This approach is most beneficial because the fuzzy rule base can be updated with ease when new data sets are available [70]. A new rule is created for any new set of available data pairs, followed by updating of the fuzzy rule base by this new rule (see Figure 6).

The learning phase of the neurofuzzy model in the HyFIS employs a gradient descent learning algorithm-based MLP network for adapting the fuzzy model parameters [71]. The model structure simplifies knowledge acquisition, approximate reasoning, and learning from data; it allows the use of both fuzzy rules and numerical data which brings about the benefits of the two data sources. In the HyFIS, the proposed neurofuzzy model is a multilayered ANN that combined numerous fuzzy systems. As captured in Figure 6, there are five layers in the system. In this structure, the input node is the input state signal while the output node is the output control/decision signal. The MFs and the rules are represented by the nodes in the hidden layers.

The nodes in the first layer are the inputs; their major role is input signals transmitted to the next layer. The second and fourth layers have the term nodes that serve as MFs for the input-output fuzzy linguistic variables expression. The fuzzy sets defined in this layer for the input-output variables are denoted as large (L), medium (M), and small (S). For the third layer, each of the nodes is a rule node that represents only one fuzzy rule. The certainty factor of the associated rules between Layers 4 and 5 is represented by the connection weights between the layers, meaning that the weight values control the level of activation of each rule. Finally, the
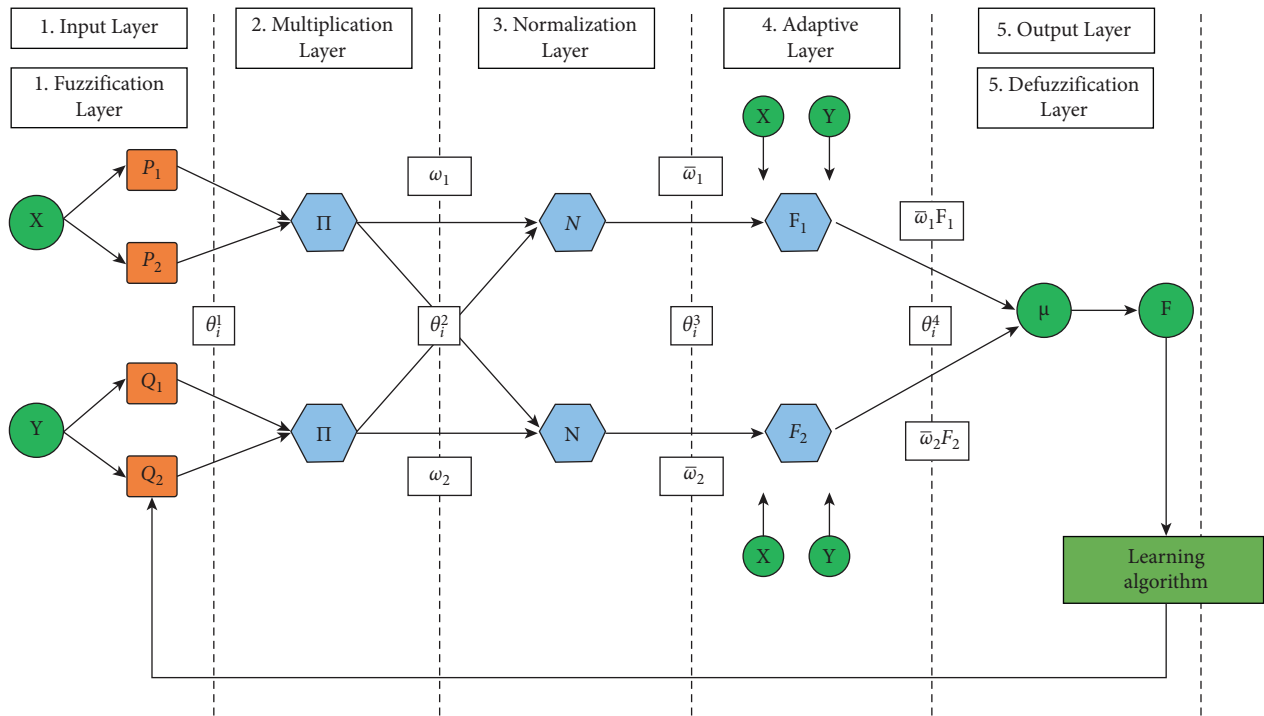
FIGURE 5: A schematic diagram for working flow of the ANFIS algorithm for the specific dataset.
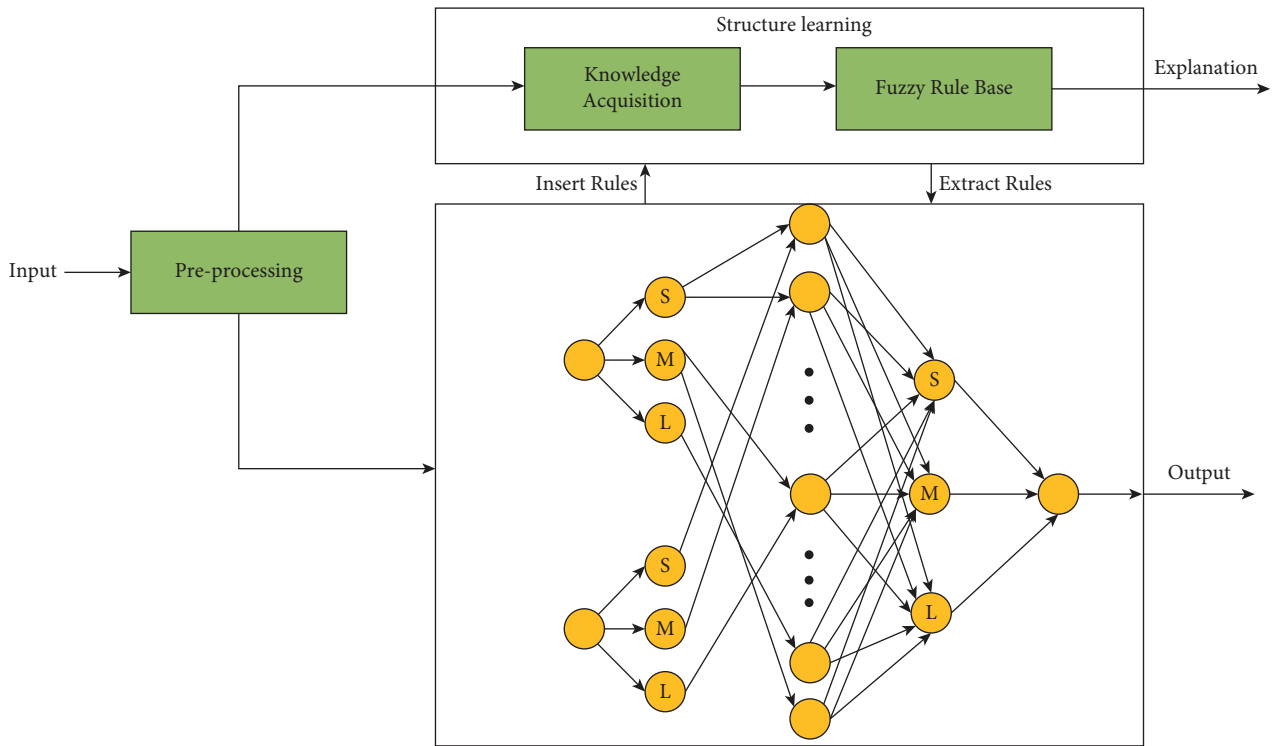

FIGURE 6: A schematic diagram for working flow of the HyFIS algorithm for the specific dataset.

nodes that represent the system's output are the nodes of the fifth layer.

2.3. Performance Metrics. Model competence and performance can be measured based on numerous metrics. Various performance metrics have been employed for assessing river WQ data modelling in the past two decades [72]. To gain more insight into the model performance, it is important to include the goodness of fit and absolute error measures [73]. This study applied seven commonly used metrics which are coefficient of determination (R^2), root-mean-squared error (RMSE), Nash-Sutcliffe efficiency (NSE), modified index of agreement (md), mean absolute error (MAE), and mean absolute percentage error (MAPE) [74–76] as represented in equations (7)–(12):

$$R^2 = 1 - \frac{\sum (a_i - p_i)^2}{\sum (a_i - \mu_a)^2}, \tag{7}$$

$$RMSE = \sqrt{\frac{1}{n} \sum_{i=1}^{n} (a_i - p_i)^2}, \tag{8}$$

$$NSE = 1 - \frac{\sum^n (\widehat{a}_i - p_i)^2}{\sum (p_i - \overline{Y})^2}, \tag{9}$$

$$md = 1.0 - \frac{\sum_{i=1}^{n} |p_i - a_i|}{\sum_{i=1}^{n} |a_i - \overline{p}| + |p_i - \overline{p}|}, \tag{10}$$

$$MAE = \frac{1}{n} \sum_{i=1}^{n} |a_i - p_i|, \tag{11}$$

$$MAPE = \sum_{i=1}^{n} |(p_i - a_i) \div a_i| \times 100 \div n, \tag{12}$$

where n is the total number of data: a denotes the output values, p denotes the real values, and μ_a is the mean value of the values, and n is the number of observations. In the current research, several statistical metrics were computed to have a more informative visualization of the applied predictive models. This is due to the limitation of some statistics such as RMSE which does not provide a sufficient error distribution. Hence, investigating more than one couple of statistical metrics can provide a more comprehensive prediction evaluation.

R software has been used for building the applied models and the statistical measurement. The applied libraries are caret, plyr, recipes, dplyr, hydroGOF, and zoo. The method CV and LOOCV have been applied. The best values of the hyperparameters have been selected.

3. Application Results and Analysis

3.1. Robinson Station. Each model performed differently based on the dataset gathered from each station. Model performance can be evaluated at different levels such as accuracy

or error generated by the models. As shown in Figure 7(a), the boxplot presents the relative error (RE) produced by the three models and it can be observed that the DENFIS result shows median RE value nearest to zero with the least number of outliers. On the other hand, even though ANFIS generated an RE value closest to zero, it produced a lot of outliers in the lower quartile area. However, in the case of HyFIS, results show a high amount of RE, a huge deviation from zero, and extended whiskers due to a lot of outliers. In terms of correlation and standard deviation results, DENFIS scored the best and is thus the nearest to the actual value as presented in Figure 7(b), followed by ANFIS and HyFIS models. Updating the cluster partition using step in case of DENFIS makes it stands at the top. Furthermore, it can be concluded that DENFIS is capable of producing fewer errors in terms of RMSE: 4.031 MAE: 3.077, and MAPE: 0.159, whereas ANFIS and HyFIS generated more errors of RMSE: 5.142 and 7.271, MAE: 3.870 and 5.954, and MAPE: 0.354 and 0.277, respectively (see Table 2).

3.2. Ada Station. In the Ada station, it can be observed that the model behaviour is slightly different than the results observed in the Robinson station. The error produced by the model has a huge impact on the overall performance and as per the RMSE values, DENFIS can produce the least error and then ANFIS and HyFIS, i.e., 4.979, 5.502, and 7.025, respectively. Similarly, when testing the A_T predicting error, the MA error values were highest for HyFIS and then ANFIS and lowest for DENFIS, i.e., 5.666, 4.129, and 3.729, respectively (see Table 3). Similarly, RE values presented as a boxplot in Figure 9(a) show the deviation of the RE produced by the models from the desired value, zero. Unlike the previous model RE performance (i.e., Robinson station), all three models generated values near zero; however, all produced outliers in the low quartile of the sample population. When ranked, HyFIS show higher percentage samples in the lower quartile and similarly more outliers leading to be ranked as last whereas sample population distribution was more equally distributed for DENFIS, including the outliers. The overall model performance correlation assessment can be done using Taylor diagram in Figure 9(b) where DENFIS and ANFIS show almost the same correlation and slight diffidence compared to standard deviation results from the actual value.

To estimate the robustness and accuracy of the model in prediction A_T, Nash metrics were estimated. As presented in Table 3, DENFIS outperformed ANFIS and HyFIS with Nash values of 0.952, 0.941, and 0.904, respectively. However, Nash is sensitive to outliers; thus, it is relevant to measure the model performance with other metrics such as R^2 and Md. As visualized in Figures 10(a)–10(c), DENFIS showed best-fit values when the scatter plot was done with an R^2 value of 0.953; ANFIS showed little variation from the trend line with an R^2 value of 0.943; on the contrary, the HyFIS plot was more dispersed with an R^2 value of 0.908. In the case of DENFIS, the creation of a new rule upon the establishment of a new cluster, followed by the creation of the new consequent part, made it outperform ANFIS and HyFIS.
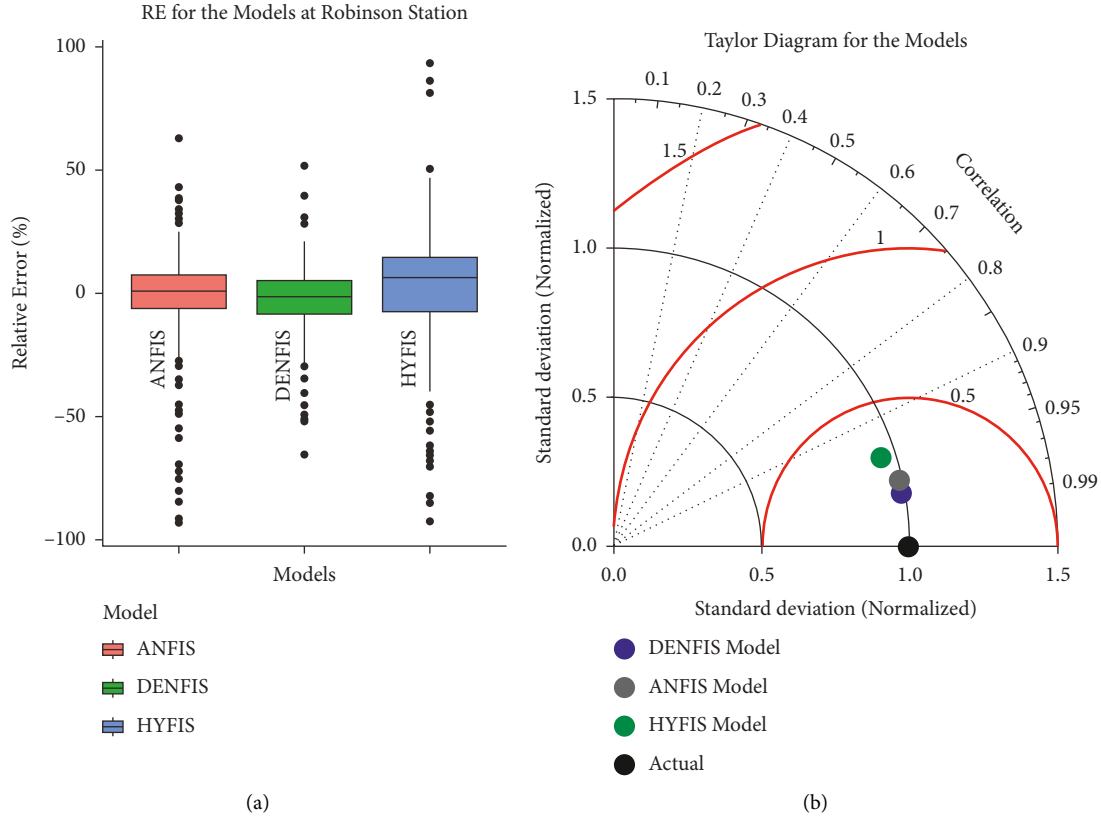
(a)

(b)

FIGURE 7: (a) Boxplot of residual error produced by all the models at Robinson station; (b) Taylor diagram with the comparative performance of the models at Robinson station.

TABLE 2: Performance metrics at Robinson station for A_T modelling.

Models	R^2	RMSE	MAE	MAPE	Nash	MD
			Training			
DENFIS	**0.971**	**4.082**	**3.076**	**0.134**	**0.971**	**0.923**
ANFIS	0.949	5.485	4.225	0.370	0.947	0.894
HyFIS	0.919	7.157	5.769	0.312	0.909	0.856
Models	*R^2*	*RMSE*	*MAE*	*Testing*	*Nash*	*MD*
			MAPE			
DENFIS	**0.968**	**4.031**	**3.077**	**0.159**	**0.968**	**0.919**
ANFIS	0.949	5.142	3.870	0.354	0.949	0.899
HyFIS	0.904	7.271	5.954	0.277	0.897	0.845

It can be observed from the training and validation result evaluation that DENFIS outperformed others, and ANFIS performance was a little behind DENFIS; nonetheless, HyFIS performance improved from the training to validation phase in terms of error production with MAPE decreased from 0.961 to 0.375 and accuracy of MD was improved from 0.797 to 0.845. For the Ada station dataset, DENFIS is the highest performing model and ANFIS is a good and robust model.

3.3. Hillsboro Station. The model error rate for the Hillsboro dataset for A_T prediction showed a similar pattern as discussed for other stations and DENFIS and ANFIS mean values were near zero in comparison to HyFIS. Figure 11(a) clearly shows that HyFIS sample population distribution is skewed and more deviated towards the lower quadrant. It can be observed that when dealing with this dataset the model produced lots of outliners in both extents of the quadrants. Furthermore, when Figure 11(b) is perceived, it is apparent that the Taylor diagram shows that DENFIS is exceedingly correlated with actual value, even though ANFIS is not far behind.

In terms of accuracy, Figure 12 was able to specify the individual performance of the model when predicting A_T. Figures 12(a) and 12(b) evaluations show that the values are near the trend line and among all DENFIS show the best fit with R^2 of 0.960. Contrarily, HyFIS shows a more random and disorganized pattern and is away from the trend line (see Figure 12(c)). This result can be supported by the evaluation results produced by Nash and Md as in Table 4. DENFIS accuracy was highest with Nash: 0.960 and MD: 0.912, followed by ANFIS and HyFIS with Nash: 0.941 and 0.873 and MD: 0.890 and 821, respectively. Regarding the other error metrics such as RMSE, MAE, and MAPE, HyFIS generated the maximum number of errors during the prediction with RMSE: 8.162, MAE: 6.693, and MAPE: 1.716. On the contrary, the error caused by the DENFIS and ANFIS was almost 50% less than HyFIS concerning MAE and RMSE.

In the overall assessment between testing and training runs, DENFIS and ANFIS gave similar results except for the
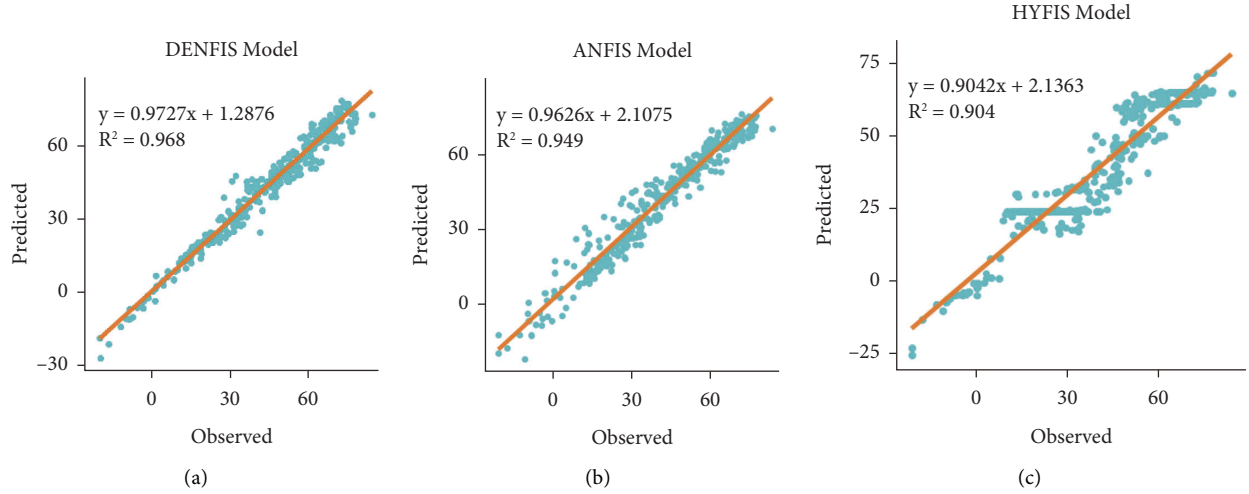
FIGURE 8: Scatter plot for (a) DENFIS; (b) ANFIS; (c) HyFIS models at Robinson station.

TABLE 3: Performance metrics at Ada station for A_T modelling.

Models	Training					
	R^2	RMSE	MAE	MAPE	Nash	MD
DENFIS	**0.963**	**4.671**	**3.454**	0.229	**0.963**	**0.916**
ANFIS	0.949	5.852	4.392	0.333	0.942	0.889
HyFIS	0.821	10.320	7.914	0.961	0.821	0.797
Models	Testing					
	R^2	RMSE	MAE	MAPE	Nash	MD
DENFIS	**0.953**	**4.979**	**3.729**	0.319	**0.952**	**0.903**
ANFIS	0.943	5.502	4.129	**0.270**	0.941	0.889
HyFIS	0.908	7.025	5.666	0.375	0.904	0.845

MAPE value of DENFIS. MAPE was much higher in a testing run but other errors were slightly less. DENFIS generated RMSE: 4.596, MAE: 3.417, and MAPE: 0.734 followed by ANFIS with RMSE: 5.578, MAE: 4.161 and little more MAP (1.707) error in comparing the other two errors for evaluation. The error devised by MAPE can be due to the high forecast in this study and since MAPE has no upper limit it can sometimes lead to difficulty in the assessment. The marginal uplifted value by DENFIS might be due to updating of the linear parameters upon the creation of a new cluster, following carrying out the required adaptation of the related parameters.

4. Discussion and Comparative Analysis

Among all stations, the DENFIS model worked well for Robinson and possibly applied the Willmott formula to overcome the issues created by the presence of the outliers in the dataset and the lower correlation in case of WS and the marginal difference in case of DP and TSR. Also, it has been observed that ANFIS worked better than HyFis in the case of Ada and Hillsboro due to a lower correlation with WS; so an upper than 27 in negative relation makes ANFIS work better. Few previous studies have been done where A_T was predicted using other models and has been discussed in this study to

assess the possible future aspect of utilizing FIS type of models. A study conducted by Karthika and Deka [77] predicted A_T by applying wavelet-ANFIS and ANFIS at Bhadra station, Karnataka, India. The result showed the highest R^2: 0.95 for Db4 Gauss wavelet-ANFIS, and ANFIS produced poor performance, i.e., R^2: 0.39. On the contrary, in this study, DENFIS performed the best with R^2: 0.953–0.968 and for ANFIS R^2 was 0.942–0.949.

Similarly, another study reported the prediction of minimum, mean, and maximum AT over southwest Asia by applying ANFIS with genetic algorithm (GA), particle swarm optimization (PSO), and ant colony optimization for continuous domains (ACOR), and differential evolution (DE). The performance of these models, i.e., ANFIS, ANFIS-ACOR, ANFIS-GA, ANFIS-DE, and ANFIS-PSO in predicting max AT in terms of R^2 was 0.88, 0.95, 0.93, 0.94, and 0.90, and for min AT the R^2 were 0.72, 0.93, 0.93, 0.93, and 0.93, and for mean AT R^2 were 0.55, 0.88, 0.92, 0.90, and 0.91 [78]. It is evident from this hybrid ANFIS model that performance varied between 0.88 and 0.95 and the conventional ANFIS performance fluctuated between 0.55 and 0.88; at the same time, the ANFIS model in this study performed between 0.942 and 0.949 which shows the model accuracy was considerably improved in the current research. In addition to that, the new model DENFIS and HyFIS also performed well when handling different datasets, i.e., R^2 0.953–0.968 and 0.904–0.908, respectively. Another study set ANFIS (R^2 0.945) better than the dynamic thermal exchange model, i.e., energy balance equation (EBE) (R^2 0.743), respectively, with the small size data, though this research suits the reliable proposing DENFIS along with ANFIS and HyFIS [79]. Moreover, [80] reported that the SVR (R^2 0.95) outperformed the ANN model too with the limited scenarios of the applied data, where the current research fills the gap by performing those adequately created scenarios to set the reliable application of the DENFIS to the real world. Those overcome could be possible due to several possible advantages of the DENFIS algorithm such as fuzzy rules that are generated, meaning that only the MFs parameters are
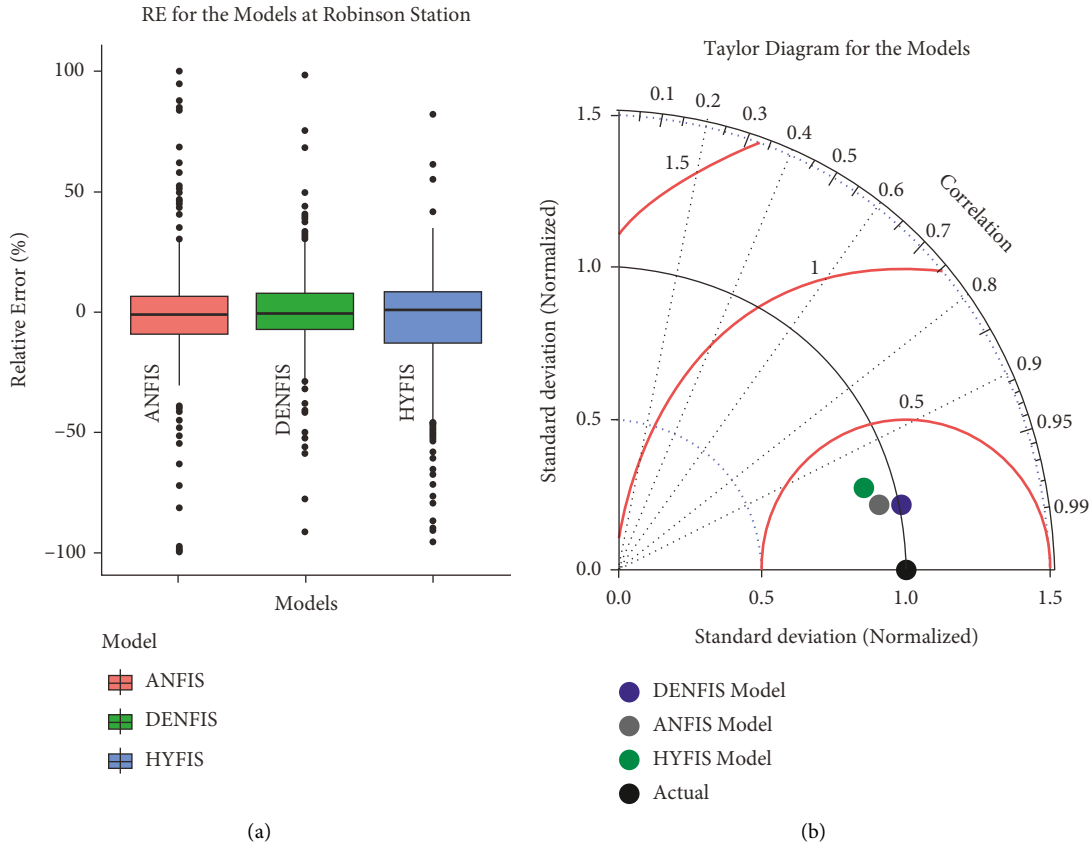
(a)

(b)

FIGURE 9: (a) Boxplot of residual error produced by all the models at Ada station; (b) Taylor diagram with the comparative performance of the models at Ada station.
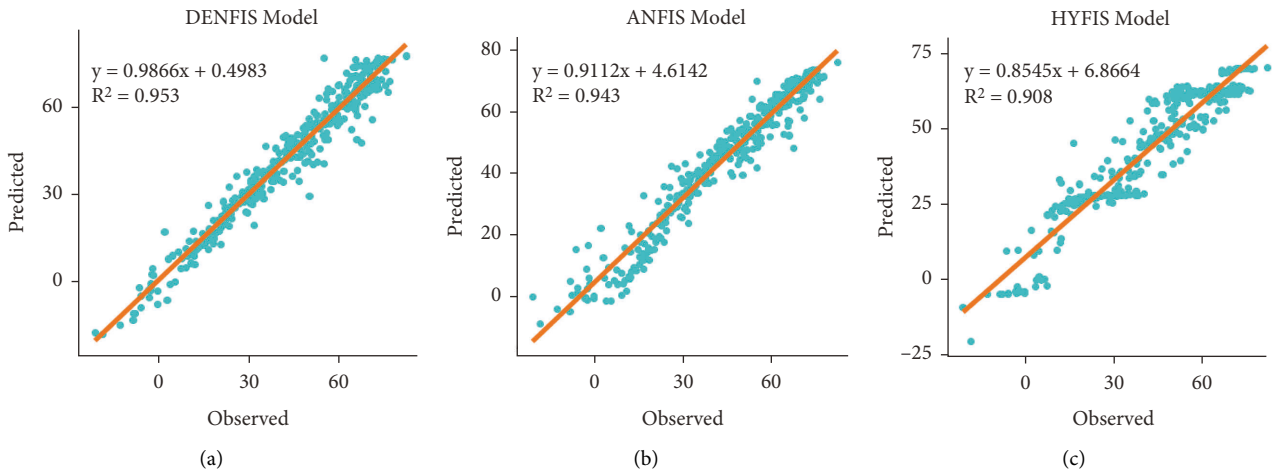

(a)

(b)

(c)

FIGURE 10: Scatter plot for (a) DENFIS; (b) ANFIS; (c) HyFIS models at Ada station.

calculated adequately and the activated rules for the fuzzy rules with the best performance have been investigated. Recently, [81] reported the ANFIS and DENFIS with a marginal difference using short-ranged data (of soil moisture) compared with the current study using long-ranged data. The authors also mentioned that ANFIS (step size: 0.001, membership type: Gaussian) and DENFIS (Max

iteration: 3000, Step size: 0.01) were overcome with the HyFIS architect. Also, the Gaussian membership function of ANFIS remains the best performer. Another study reveals that the hybridization of DENFIS with two advanced metaheuristic optimization algorithms (i.e., Whale Optimization Algorithm (WOA) and Bat Algorithm (BA)) showed the potential predictive capacity as per the R^2
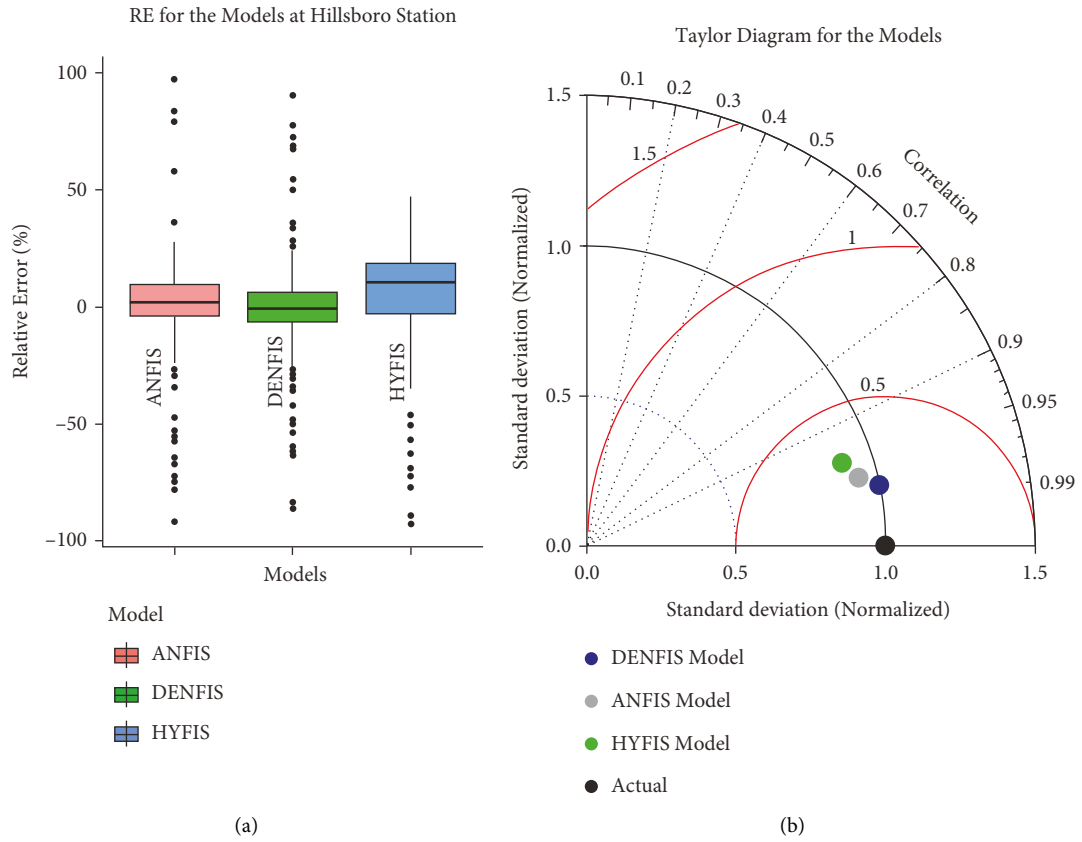
(a)

(b)

FIGURE 11: (a) Boxplot of residual error for models at Hillsboro station; (b) Taylor diagram of models at Hillsboro station.

(a)

(b)

(c)
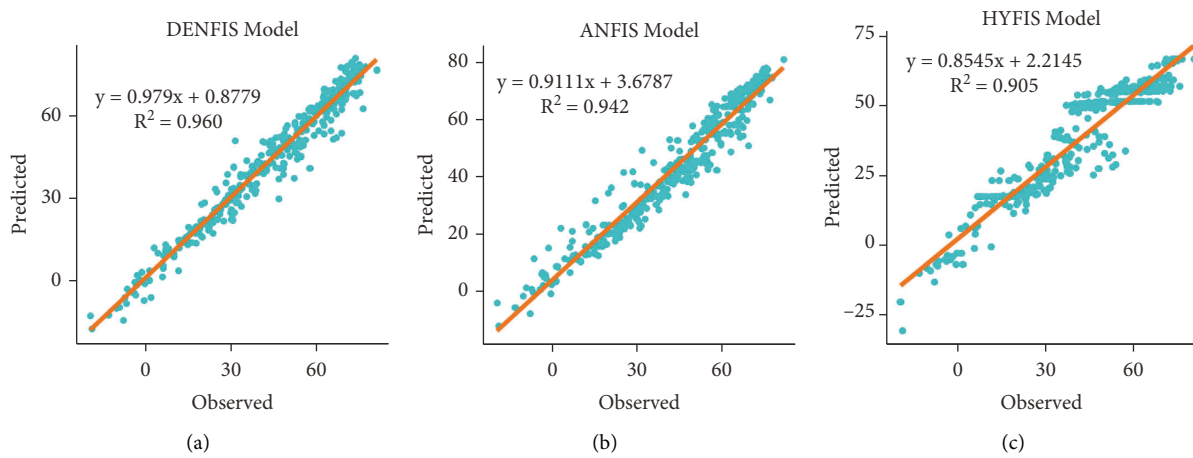
FIGURE 12: Scatter plot for (a) DENFIS; (b) ANFIS; (c) HyFIS models at Hillsboro station.

TABLE 4: Performance metrics at Hillsboro station for A_T modelling.

Models	R^2	RMSE	MAE	MAPE	Nash	MD
			Training			
DENFIS	**0.964**	**4.672**	**3.457**	**0.217**	**0.964**	**0.917**
ANFIS	0.946	5.924	4.504	0.658	0.941	0.888
HyFIS	0.917	8.373	6.760	0.338	0.883	0.831
			Testing			
Models	*R^2*	*RMSE*	*MAE*	*MAPE*	*Nash*	*MD*
DENFIS	**0.960**	**4.596**	**3.417**	**0.734**	**0.960**	**0.912**
ANFIS	0.942	5.578	4.161	1.707	0.941	0.890
HyFIS	0.905	8.162	6.693	1.716	0.873	0.821

(0.85–0.94) against the counterpart MARS to predict the daily scale evapotranspiration for three different coastal locations [46].

5. Conclusion

The current research reviewed the prediction competencies of advanced FIS type models such as DENFIS, ANFIS, and HyFIS. The models were able to successfully predict AT (target variable) with high accuracy and less error while using only three input variables, i.e., DP, TSR, and WS. The models were applied for three datasets acquired from three stations in North Dakota, USA, i.e., Robinson, Ada, and Hillsboro, from 2015 to 2019. Among the three applied models, DENFIS outperformed the others, followed by ANFIS and HyFIS for all three stations. The performance efficiency of DENFIS in Robinson, Ada, and Hillsboro stations was excellent with R^2: 0.97/0.95/0.96, RMSE: 4.0/4.9/4.6, and md: 0.91/0.90/0.92, respectively. Following DENFIS results, ANFIS also performed well with R^2: 0.95/0.94/0.94, RMSE: 5.1/5.5/5.6, and md: 0.90/0.89/0.89, respectively. Lastly, HyFIS similarly performed well with R^2: 0.90/0.90/0.87, RMSE: 7.3/7.0/8.2, and md: 0.84/0.79/0.82, respectively. North Dakota has reported significantly several AT complementary relations with other parameters of the sciences and engineering; for example, the evapotranspiration has been increasing over the period [82], in borehole paleoclimatology directly linked with AT [83], and snowpack control alteration [84], which lead many challenging to resources management. A report says that the lower-income area has much potential for green emission of air pollution [85]. The study is helpful to design the accurate decision priory and appropriately as per the local geographical location. Even the study applied the black box type models which have their limitations; however, they can simplify the assessment and prediction method when dealing with the meteorological data which plays an imperative role in various environmental, climatological, and meteorological studies. One of the current burning topics in these fields is climate change and such studies which applied ML methods for data modelling with similar statistical characteristics should be studied more to make a more precise projection of the future changes which will change the Earth environment. It is worth mentioning that more research should be done considering different geological conditions, diverse model types, and various diverse input variables. Also, another different meteorological parameter can be used to support the sustainable water resources and agricultural systems.

Data Availability

Data can be shared upon request from the corresponding author.

Conflicts of Interest

The authors declare no conflicts of interest in this study

References

[1] M. C. Thomson, S. J. Connor, P. J. M. Milligan, and S. P. Flasse, "The ecology of malaria—as seen from Earth-observation satellites," *Annals of Tropical Medicine and Parasitology*, vol. 90, no. 3, pp. 243–264, 1996.

[2] S. J. Goetz, S. D. Prince, and J. Small, "Advances in satellite remote sensing of environmental variables for epidemiological applications," *Advances in Parasitology*, vol. 47, pp. 289–307, 2000.

[3] C. J. Kucharik, S. P. Serbin, S. Vavrus, E. J. Hopkins, and M. M. Motew, "Patterns of climate change across Wisconsin from 1950 to 2006," *Physical Geography*, vol. 31, no. 1, pp. 1–28, 2010.

[4] D. Bocchiola and G. Diolaiuti, "Evidence of climate change within the adamello glacier of Italy," *Theoretical and Applied Climatology*, vol. 100, no. 3–4, pp. 351–369, 2010.

[5] B. Halder, M. Haghbin, and A. A. Farooque, "An assessment of urban expansion impacts on land transformation of rajpur-sonarpur municipality," *Knowledge-Based Engineering and Sciences*, vol. 2, no. 3, pp. 34–53, 2021.

[6] L. Bian, L. Li, and G. Yan, "Combining global and local estimates for spatial distribution of mosquito larval habitats," *GIScience and Remote Sensing*, vol. 43, no. 2, pp. 128–141, 2006.

[7] A. Sharafati, K. Khosravi, P. Khosravinia et al., "The potential of novel data mining models for global solar radiation prediction," *International journal of Environmental Science and Technology*, vol. 16, no. 11, pp. 7147–7164, 2019.

[8] N. A. Brunsell, D. B. Mechem, and M. C. Anderson, "Surface Heterogeneity Impacts on Boundary Layer Dynamics via Energy Balance Partitioning," *Atmospheric Chemistry and Physics*, vol. 11, 2011.

[9] K. Aasamaa and A. Sõber, "Stomatal sensitivities to changes in leaf water potential, air humidity, CO_2 concentration and light intensity, and the effect of abscisic acid on the sensitivities in six temperate deciduous tree species," *Environmental and Experimental Botany*, vol. 71, no. 1, pp. 72–78, 2011.

[10] B. Bickici Arikan, L. Jiechen, I. Sabbah, A. Ewees, R. Homsi, and S. O. Sulaiman, "Dew point time series forecasting at the north Dakota," *Knowledge-Based Engineering and Sciences*, vol. 2, no. 2, pp. 24–34, 2021.

[11] S. W. Myint, A. Brazel, G. Okin, and A. Buyantuyev, "Combined effects of impervious surface and vegetation cover on air temperature variations in a rapidly expanding desert city," *GIScience and Remote Sensing*, vol. 47, no. 3, pp. 301–320, 2010.

[12] L. C. Smith, "Agents of change in the new north," *Eurasian Geography and Economics*, vol. 52, no. 1, pp. 30–55, 2011.

[13] S. Heding, L. Kai, C. Hanchun, C. Xianlong, H. Yongan, and S. Zhiyi, "Experimental ecology and hibernation of onchidium struma (gastropoda: pulmonata: systellommatophora)," *Journal of Experimental Marine Biology and Ecology*, vol. 396, no. 2, pp. 71–76, 2011.

[14] Z. M. Yaseen, T. T. Zigale, S. Q. Salih et al., "Laundry wastewater treatment using a combination of sand filter, biochar and teff straw media," *Scientific Reports*, vol. 9, no. 1, pp. 18709–18711, 2019.

[15] S. K. Bhagat, Tiyasha, and D. N. Bekele, "Economical approaches for the treatment and Re utilization of laundry wastewater - a review," *Journal of Industrial Pollution Control*, vol. 34, no. 2, pp. 2164–2178, 2018.

[16] S. K. Bhagat and Tiyasha, "Impact of millions of tones of effluent of textile industries: analysis of textile industries effluents in Bhilwara and an approach with bioremediation," *International Journal of ChemTech Research*, vol. 5, no. 3, pp. 1289–1298, 2013.

[17] S. K. Jain, S. K. Jain, V. Hariprasad, and A. Choudhry, "Water balance study for a basin integrating remote sensing data and GIS," *Journal of the Indian Society of Remote Sensing*, vol. 39, no. 2, pp. 259–270, 2011.

[18] S. Cheval, A. Dumitrescu, and A. Bell, "The urban heat island of Bucharest during the extreme high temperatures of July 2007," *Theoretical and Applied Climatology*, vol. 97, no. 3–4, pp. 391–401, 2009.

[19] M. Xu, S. Kang, H. Wu, and X. Yuan, "Detection of spatio-temporal variability of air temperature and precipitation based on long-term meteorological station observations over Tianshan Mountains, Central Asia," *Atmospheric Research*, vol. 203, pp. 141–163, 2018.

[20] S. Sim, J. Im, S. Park, H. Park, M. H. Ahn, and P. W. Chan, "Icing detection over East Asia from geostationary satellite data using machine learning approaches," *Remote Sensing*, vol. 10, no. 4, p. 631, 2018.

[21] C. Yoo, D. Han, J. Im, and B. Bechtel, "Comparison between convolutional neural networks and random forest for local climate zone classification in mega urban areas using Landsat images," *ISPRS Journal of Photogrammetry and Remote Sensing*, vol. 157, pp. 155–170, 2019.

[22] K. Ahmed, D. A. Sachindra, S. Shahid, Z. Iqbal, N. Nawaz, and N. Khan, "Multi-model ensemble predictions of precipitation and temperature using machine learning algorithms," *Atmospheric Research*, vol. 236, Article ID 104806, 2020.

[23] R. C. Deo and M. Şahin, "Application of the extreme learning machine algorithm for the prediction of monthly Effective Drought Index in eastern Australia," *Atmospheric Research*, vol. 153, pp. 512–525, 2015.

[24] S. K. Bhagat, T. Tiyasha, T. M. Tung, R. R. Mostafa, and Z. M. Yaseen, "Manganese (Mn) removal prediction using extreme gradient model," *Ecotoxicology and Environmental Safety*, vol. 204, Article ID 111059, 2020.

[25] R. F. Chevalier, G. Hoogenboom, R. W. McClendon, and J. A. Paz, "Support vector regression with reduced training sets for air temperature prediction: a comparison with artificial neural networks," *Neural Computing & Applications*, vol. 20, no. 1, pp. 151–159, 2011.

[26] Q. Fang, Z. Li, Y. Wang, M. Song, and J. Wang, "A neural-network enhanced modeling method for real-time evaluation of the temperature distribution in a data center," *Neural Computing & Applications*, vol. 31, no. 12, pp. 8379–8391, 2019.

[27] C. Marzban, "Neural networks for postprocessing model output: ARPS," *Monthly Weather Review*, vol. 131, no. 6, pp. 1103–1111, 2003.

[28] A. Jain, R. W. McClendon, G. Hoogenboom, and R. Ramyaa, "Prediction of Frost for Fruit protection Using Artificial Neural Networks," *The American Society of Agricultural and Biological Engineers*, pp. 3–3075, 2003.

[29] J.-D. Jang, A. A. Viau, and F. Anctil, "Neural network estimation of air temperatures from AVHRR data," *International Journal of Remote Sensing*, vol. 25, no. 21, pp. 4541–4554, 2004.

[30] B. A. Smith, R. W. McClendon, and G. Hoogenboom, "Improving air temperature prediction with artificial neural networks," *International Journal of Computational Intelligence*, vol. 3, no. 3, pp. 179–186, 2006.

[31] S. Salcedo-Sanz, R. C. Deo, L. Carro-Calvo, and B. Saavedra-Moreno, "Monthly prediction of air temperature in Australia and New Zealand with machine learning algorithms," *Theoretical and Applied Climatology*, vol. 125, no. 1-2, pp. 13–25, 2015.

[32] E. Eccel, L. Ghielmi, P. Granitto, R. Barbiero, F. Grazzini, and D. Cesari, "Prediction of Minimum Temperatures in an alpine Region by Linear and Non-linear post-processing of Meteorological Models," *Nonlinear Processes in Geophysics*, vol. 14, 2007.

[33] B. A. Smith, G. Hoogenboom, and R. W. McClendon, "Artificial neural networks for automated year-round temperature prediction," *Computers and Electronics in Agriculture*, vol. 68, no. 1, pp. 52–61, 2009.

[34] S. Vashani, M. Azadi, and S. Hajjam, "Comparative Evaluation of different post processing methods for numerical prediction of temperature forecasts over Iran," *Research Journal of Environmental Sciences*, vol. 4, no. 3, pp. 305–316, 2010.

[35] M. Şahin, "Modelling of air temperature using remote sensing and artificial neural network in Turkey," *Advances in Space Research*, vol. 50, no. 7, pp. 973–985, 2012.

[36] O. Kisi and J. Shiri, "Prediction of long-term monthly air temperature using geographical inputs," *International Journal of Climatology*, vol. 34, no. 1, pp. 179–186, 2014.

[37] L. Penghui, A. A. Ewees, B. H. Beyaztas et al., "Metaheuristic optimization algorithms hybridized with artificial intelligence model for soil temperature prediction: novel model," *IEEE Access*, vol. 8, pp. 51884–51904, 2020.

[38] A. Sharafati, M. Haghbin, M. S. Aldlemy et al., "Development of advanced computer aid model for shear strength of concrete slender beam prediction," *Applied Sciences*, vol. 10, no. 11, p. 3811, 2020.

[39] C. Yi, Y. Shin, and J.-W. Roh, "Development of an urban high-resolution air temperature forecast system for local weather information services based on statistical downscaling," *Atmosphere*, vol. 9, no. 5, p. 164, 2018.

[40] J.-Y. Shin, K. R. Kim, and J.-C. Ha, "Seasonal forecasting of daily mean air temperatures using a coupled global climate model and machine learning algorithm for field-scale agricultural management," *Agricultural and Forest Meteorology*, vol. 281, Article ID 107858, 2020.

[41] D. Cho, C. Yoo, J. Im, and D. Cha, "Comparative assessment of various machine learning-based bias correction methods for numerical weather prediction model forecasts of extreme air temperatures in urban areas," *Earth and Space Science*, vol. 7, no. 4, 2020.

[42] S. Heddam and N. Dechemi, "A New Approach Based on the Dynamic Evolving Neural-Fuzzy Inference System (DENFIS) for Modelling Coagulant Dosage (Dos): Case Study of Water Treatment Plant of Algeria," *Desalin. Water Treat*, vol. 53, 2015.

[43] O. Eray, C. Mert, and O. Kisi, "Comparison of multi-gene genetic programming and dynamic evolving neural-fuzzy inference system in modeling pan evaporation," *Hydrology Research*, vol. 49, no. 4, pp. 1221–1233, 2017.

[44] A. Talei, L. H. C. Chua, and C. Quek, "Hydrological modelling with a dynamic neural fuzzy inference system," in *HIC 2012: Understanding Changing Climate and Environment and Finding Solutions: Proceedings of the 10th International Conference on Hydroinformatics* p. 1, Hamburg, Germany, 2012.

[45] A. Anand, A. S. Dinesh, P. K. Srivastava, S. K. Chaudhary, A. K. Varma, and P. Kumar, "Rainfall rate estimation over

India using global precipitation measurement's microwave imager datasets and different variants of fuzzy information system," *Geocarto International*, pp. 1–19, 2021.

[46] L. Ye, M. M. A. Zahra, N. K. Al-Bedyry, and Z. M. Yaseen, "Daily scale evapotranspiration prediction over the coastal region of southwest Bangladesh: new development of artificial intelligence model," *Stochastic Environmental Research and Risk Assessment*, vol. 36, no. 2, pp. 451–471, 2022.

[47] E. K. Mustafa, Y. Co, G. Liu et al., "Study for predicting land surface temperature (LST) using landsat data: a comparison of four algorithms," *Advances in Civil Engineering*, vol. 2020, Article ID 7363546, 16 pages, 2020.

[48] K. B. Dang, B. Burkhard, W. Windhorst, and F. Müller, "Application of a hybrid neural-fuzzy inference system for mapping crop suitability areas and predicting rice yields," *Environmental Modelling & Software*, vol. 114, pp. 166–180, 2019.

[49] A. Jozi, T. Pinto, I. Praça, F. Silva, B. Teixeira, and Z. Vale, "Energy consumption forecasting based on hybrid neural fuzzy inference system," in *Proceedings of the 2016 IEEE Symposium Series on Computational Intelligence (SSCI)*, pp. 1–5, Athens, Greece, December 2016.

[50] R. Li and J. W. Merchant, "Modeling vulnerability of groundwater to pollution under future scenarios of climate change and biofuels-related land use change: a case study in North Dakota, USA," *Science of the Total Environment*, vol. 447, pp. 32–45, 2013.

[51] USGCRP, *The Impacts of Climate Change on Human Health in the United States: A Scientific Assessment*, U.S. Global Change Research Program, Washington, DC, USA, 2016.

[52] N. K. Kasabov and Q. Song, "DENFIS: dynamic evolving neural-fuzzy inference system and its application for time-series prediction," *IEEE Transactions on Fuzzy Systems*, vol. 10, no. 2, pp. 144–154, 2002.

[53] A. Amirkhani, H. Nasiriyan-Rad, and E. I. Papageorgiou, "A novel fuzzy inference approach: neuro-fuzzy cognitive map," *International Journal of Fuzzy Systems*, vol. 22, no. 3, pp. 859–872, 2020.

[54] N. Kasabov, *Evolving Connectionist Systems: The Knowledge Engineering Approach*, Springer Science \& Business Media, Berlin, Germany, 2007.

[55] M. J. Watts, "A Decade of Kasabov's Evolving Connectionist Systems: A Review," *IEEE Transactions on Systems, Man, and Cybernetics - Part C: Applications and Reviews*, vol. 39, 2009.

[56] T. Takagi and M. Sugeno, "Fuzzy identification of systems and its applications to modeling and control," *IEEE Transactions on Systems, Man, and Cybernetics*, vol. 15, no. 1, pp. 116–132, 1985.

[57] H. Tao, A. A. Ewees, A. O. Al-Sulttani et al., "Global solar radiation prediction over North Dakota using air temperature: development of novel hybrid intelligence model," *Energy Reports*, vol. 7, pp. 136–157, 2021.

[58] N. K. Kasabov, "Evolving connectionist systems for adaptive learning and knowledge discovery: trends and directions," *Knowledge-Based Systems*, vol. 80, pp. 24–33, 2015.

[59] E. Lughofer, "EFS approaches for regression and classification," in *Evolving Fuzzy Systems--Methodologies, Advanced Concepts and Applications* pp. 94–164, Berlin, Heidelberg, 2011.

[60] S. Kar, S. Das, and P. K. Ghosh, "Applications of neuro fuzzy systems: a brief review and future outline," *Applied Soft Computing*, vol. 15, pp. 243–259, 2014.

[61] J.-S. Jang, "ANFIS: adaptive-network-based fuzzy inference system," *IEEE Trans. Syst. Man. Cybern.* vol. 23, no. 3, pp. 665–685, 1993.

[62] O. E. Omeje, H. S. Maccido, Y. A. Badamasi, and S. I. Abba, "Performance of hybrid neuro-fuzzy model for solar radiation simulation at abuja, Nigeria: a correlation based input selection technique," *Knowledge-Based Eng. Sci.* vol. 2, no. 3, pp. 54–66, 2021.

[63] M. Ko, A. Tiwari, and J. Mehnen, "A review of soft computing applications in supply chain management," *Applied Soft Computing*, vol. 10, no. 3, pp. 661–674, 2010.

[64] A. Mohiyuddin, A. R. Javed, C. Chakraborty, M. Rizwan, M. Shabbir, and J. Nebhen, "Secure cloud storage for medical IoT data using adaptive neuro-fuzzy inference system," *International Journal of Fuzzy Systems*, vol. 24, no. 2, pp. 1203–1215, 2021.

[65] R. Tur and S. Yontem, "A comparison of soft computing methods for the prediction of wave height parameters," *Knowledge-Based Engineering and Sciences*, vol. 2, no. 1, pp. 31–46, 2021.

[66] A. F. GüNeri, T. Ertay, and A. YüCel, "An approach based on ANFIS input selection and modeling for supplier selection problem," *Expert Systems with Applications*, vol. 38, no. 12, pp. 14907–14917, 2011.

[67] P. Aengchuan and B. Phruksaphanrat, "Comparison of fuzzy inference system (FIS), FIS with artificial neural networks (FIS+ ANN) and FIS with adaptive neuro-fuzzy inference system (FIS+ ANFIS) for inventory control," *Journal of Intelligent Manufacturing*, vol. 29, no. 4, pp. 905–923, 2018.

[68] J. Kim and N. Kasabov, "HyFIS: adaptive neuro-fuzzy inference systems and their application to nonlinear dynamical systems," *Neural Networks*, vol. 12, no. 9, pp. 1301–1319, 1999.

[69] W. Pedrycz and F. Gomide, *Fuzzy Systems Engineering: Toward Human-Centric Computing*, John Wiley & Sons, Hoboken, NJ, USA, 2007.

[70] L.-X. Wang and J. M. Mendel, "Generating fuzzy rules by learning from examples," *IEEE Trans. Syst. Man. Cybern.* vol. 22, no. 6, pp. 1414–1427, 1992.

[71] K. Rudd, G. D. Muro, and S. Ferrari, "A constrained back-propagation approach for the adaptive solution of partial differential equations," *IEEE Transactions on Neural Networks and Learning Systems*, vol. 25, no. 3, pp. 571–584, 2014.

[72] S. K. Bhagat, T. Tiyasha, S. M. Awadh, T. M. Tung, A. H. Jawad, and Z. M. Yaseen, "Prediction of sediment heavy metal at the Australian Bays using newly developed hybrid artificial intelligence models," *Environmental Pollution*, vol. 268, Article ID 115663, 2021.

[73] S. K. Bhagat, T. M. Tung, and Z. M. Yaseen, "Heavy metal contamination prediction using ensemble model: case study of Bay sedimentation, Australia," *Journal of Hazardous Materials*, vol. 403, Article ID 123492, 2021.

[74] C. J. Willmott, "On the validation of models," *Physical Geography*, vol. 2, no. 2, pp. 184–194, 1981.

[75] P. Goodwin and R. Lawton, "On the asymmetry of the symmetric MAPE," *International Journal of Forecasting*, vol. 15, no. 4, pp. 405–408, 1999.

[76] J. S. Armstrong and F. Collopy, "Error measures for generalizing about forecasting methods: empirical comparisons," *International Journal of Forecasting*, vol. 8, no. 1, pp. 69–80, 1992.

[77] B. S. Karthika and P. C. Deka, "Prediction of air temperature by hybridized model (Wavelet-ANFIS) using wavelet decomposed data," *Aquat. Procedia*, vol. 4, pp. 1155–1161, 2015.

[78] A. Azad, H. Kashi, S. Farzin et al., "Novel approaches for air temperature prediction: a comparison of four hybrid evolutionary fuzzy models," *Meteorological Applications*, vol. 27, no. 1, 2019.

[79] Q. Xie, J.-Q. Ni, J. Bao, and Z. Su, "A thermal environmental model for indoor air temperature prediction and energy consumption in pig building," *Building and Environment*, vol. 161, Article ID 106238, 2019.

[80] X. Zhang, Y. Wang, X. He et al., "Prediction of vehicle driver's facial air temperature with SVR, ANN, and GRU," *IEEE Access*, vol. 10, pp. 20212–20222, 2022.

[81] S. K. Chaudhary, P. K. Srivastava, D. K. Gupta et al., "Machine learning algorithms for soil moisture estimation using Sentinel-1: model development and implementation," *Advances in Space Research*, vol. 69, no. 4, pp. 1799–1812, 2022.

[82] D. O. Rosenberry, D. I. Stannard, T. C. Winter, and M. L. Martinez, "Comparison of 13 equations for determining evapotranspiration from a prairie wetland, Cottonwood Lake area, North Dakota, USA," *Wetlands*, vol. 24, no. 3, pp. 483–497, 2004.

[83] W. L. Schmidt, W. D. Gosnold, and J. W. Enz, "A decade of air–ground temperature exchange from Fargo, North Dakota," *Global and Planetary Change*, vol. 29, no. 3–4, pp. 311–325, 2001.

[84] A. Grundstein, P. Todhunter, and T. Mote, "Snowpack control over the thermal offset of air and soil temperatures in eastern North Dakota," *Geophysical Research Letters*, vol. 32, no. 8, Article ID L08503, 2005.

[85] R. T. Carson, Y. Jeon, and D. R. McCubbin, "The relationship between air pollution emissions and income: US data," *Environment and Development Economics*, vol. 2, no. 4, pp. 433–450, 1997.